



HHS Public Access

Author manuscript

Med Phys. Author manuscript; available in PMC 2020 September 01.

Published in final edited form as:

Med Phys. 2019 September ; 46(9): 3767–3775. doi:10.1002/mp.13586.

Automated treatment planning of postmastectomy radiotherapy

Kelly Kisling,

Department of Radiation Physics, The University of Texas MD Anderson Cancer Center, Houston, Texas 77030, United States

Lifei Zhang,

Department of Radiation Physics, The University of Texas MD Anderson Cancer Center, Houston, Texas 77030, United States

Jinzhong Yang,

Department of Radiation Physics, The University of Texas MD Anderson Cancer Center, Houston, Texas 77030, United States

Peter A. Balter,

Department of Radiation Physics, The University of Texas MD Anderson Cancer Center, Houston, Texas 77030, United States

Rebecca M. Howell,

Department of Radiation Physics, The University of Texas MD Anderson Cancer Center, Houston, Texas 77030, United States

Laurence Court^{a)},

Department of Radiation Physics, The University of Texas MD Anderson Cancer Center, Houston, Texas 77030, United States

Simona F Shaitelman,

Department of Radiation Oncology, The University of Texas MD Anderson Cancer Center, Houston, Texas 77030, United States

Anuja Jhingran,

Department of Radiation Oncology, The University of Texas MD Anderson Cancer Center, Houston, Texas 77030, United States

David Anderson,

Department of Radiation Oncology, University of Cape Town and Groote Schuur Hospital, Cape Town 8000, South Africa

Tselane Thebe,

Department of Radiation Oncology, University of Cape Town and Groote Schuur Hospital, Cape Town 8000, South Africa

Kathleen Schmeler,

DISCLOSURE OF CONFLICTS OF INTEREST

This work was partially supported by Varian Medical Systems.

Department of Gynecologic Oncology and Reproductive Medicine, The University of Texas MD Anderson Cancer Center, Houston, Texas 77030, United States

Hannah Simonds,

Division of Radiation Oncology, Stellenbosch University and Tygerberg Hospital, Cape Town 7505, South Africa

Monique du Toit,

Division of Medical Physics, Stellenbosch University and Tygerberg Hospital, Cape Town 7505, South Africa

Christoph Trauernicht,

Division of Medical Physics, Stellenbosch University and Tygerberg Hospital, Cape Town 7505, South Africa

Hester Burger,

Division of Medical Physics, University of Cape Town and Groote Schuur Hospital, Cape Town 8000, South Africa

Kobus Botha,

Division of Medical Physics, University of Cape Town and Groote Schuur Hospital, Cape Town 8000, South Africa

Nanette Joubert,

Division of Medical Physics, University of Cape Town and Groote Schuur Hospital, Cape Town 8000, South Africa

Beth M. Beadle

Department of Radiation Oncology, Stanford University, Stanford, California 94305, United States

^{a)}Department of Radiation Physics, Unit 1420, The University of Texas MD Anderson Cancer Center, 1515 Holcombe Boulevard, Houston, TX 77030.

Abstract

Purpose: Breast cancer is the most common cancer in women globally and radiation therapy is a cornerstone of its treatment. However, there is an enormous shortage of radiotherapy staff, especially in low-and middle-income countries. This shortage could be ameliorated through increased automation in the radiation treatment planning process, which may reduce the workload on radiotherapy staff and improve efficiency in preparing radiotherapy treatments for patients. To this end, we sought to create an automated treatment planning tool for postmastectomy radiotherapy (PMRT).

Methods: Algorithms to automate every step of PMRT planning were developed and integrated into a commercial treatment planning system. The only required inputs for automated PMRT planning are a planning computed tomography scan, a plan directive, and selection of the inferior border of the tangential fields. With no other human input, the planning tool automatically creates a treatment plan and presents it for review. The major automated steps are (1) segmentation of relevant structures (targets, normal tissues, and other planning structures), (2) setup of the beams (tangential fields matched with a supraclavicular field), and (3) optimization of the dose distribution by using a mix of high-and low-energy photon beams and field-in-field modulation for

the tangential fields. This automated PMRT planning tool was tested with 10 computed tomography scans of patients with breast cancer who had received irradiation of the left chest wall. These plans were assessed quantitatively using their dose distributions and were reviewed by two physicians who rated them on a three-tiered scale: use as is, minor changes, or major changes. The accuracy of the automated segmentation of the heart and ipsilateral lung was also assessed. Finally, a plan quality verification tool was tested to alert the user to any possible deviations in the quality of the automatically created treatment plans.

Results: The automatically created PMRT plans met the acceptable dose objectives, including target coverage, maximum plan dose, and dose to organs at risk, for all but one patient for whom the heart objectives were exceeded. Physicians accepted 50% of the treatment plans as is and required only minor changes for the remaining 50%, which included the one patient whose plan had a high heart dose. Further, the automatically segmented contours of the heart and ipsilateral lung agreed well with manually edited contours. Finally, the automated plan quality verification tool detected 92% of the changes requested by physicians in this review.

Conclusions: We developed a new tool for automatically planning PMRT for breast cancer, including irradiation of the chest wall and ipsilateral lymph nodes (supraclavicular and level III axillary). In this initial testing, we found that the plans created by this tool are clinically viable, and the tool can alert the user to possible deviations in plan quality. The next step is to subject this tool to prospective testing, in which automatically planned treatments will be compared with manually planned treatments.

Keywords

postmastectomy radiotherapy; automated treatment planning

1. INTRODUCTION

Breast cancer is the most common cancer in women worldwide, including many low- and middle-income countries (LMICs).¹ Generally, breast cancer is diagnosed at more advanced stages in LMICs compared with more developed countries.² For breast cancer with four or more positive lymph nodes, the standard of care is postmastectomy radiotherapy (PMRT) to the chest wall and ipsilateral lymph nodes, which reduces the risk of local recurrence and improves survival.³⁻⁵ There are also increasing indications to deliver PMRT to patients with one to three positive lymph nodes or those with high-risk node negative disease, as radiation in such situations is associated with improvement in disease-free survival.⁶ Planning PMRT treatments can be difficult and time-consuming, as it involves using a complex combination of matched fields and various techniques to reduce the dose to organs at risk (OARs) and improve the homogeneity of dose to the targets. Planning such treatments is further complicated by the lack of access to technologies that facilitate deep-inspiration breath-hold techniques that reduce the dose to the heart, which is often the case in resource-constrained clinics in LMICs. These countries also have insufficient access to radiotherapy⁷ in part because of a sizable shortage in the trained staff needed to plan and deliver radiation treatment.⁸ Treatment planning constitutes a substantial amount of radiotherapy staff workload, and that workload could be reduced by increased automation. Automation is also very useful in clinics with more resources, and should help to reduce healthcare costs.

To date, most work on automating treatment planning for breast cancer has focused on a tangential field-only treatment technique or on specific steps in treatment planning, such as the inverse-planning of tangential intensity-modulated radiotherapy.^{9–13} Many of these techniques are effective and have improved the efficiency of treatment planning. Expanding from these efforts, we have developed a tool that automates the entire planning process for PMRT, which is necessary for treating more advanced breast cancers. The PMRT technique differs from the previously automated tangential field-only technique in that it includes a supraclavicular (SCV) field that is matched to tangential fields via a non-divergent border at the match line. Another unique feature of our current automation technique is that previous automation techniques require a particular placement of external fiducial markers, which is not standardized among clinics; the techniques and materials used for placing these markers vary greatly. Our goal in the present study was to develop an automated technique for planning PMRT that can be widely used at multiple institutions around the world. Thus, we designed a tool that does not require placement of external fiducial markers to determine the borders of the treatment fields.

Herein we describe the automated treatment planning tool we developed, including the techniques used for automation and the results of a planning study for patients with breast cancer who underwent PMRT. We developed this automated planning tool in a collaboration between institutions in the United States and South Africa, and it is intended for use in resource-constrained settings for radiotherapy for locally advanced breast cancer after mastectomy.

2. MATERIALS AND METHODS

2.A. Overview of the automated planning tool

The automated planning tool tested in this work designs PMRT treatments using a monoisocentric tangential and SCV field technique. To reduce the dose to OARs and improve dose homogeneity in the targets, the algorithms in this tool optimize the use of mixed high- and low-energy photon beams and, for the tangential fields, the use of field-in-field (FIF) segments. The automated planning tool was developed assuming the radiation treatments would be planned on a free-breathing computed tomography (CT) scans of patients in the head-first, supine position owing to resource limitations. The only external fiducial markers required are those indicating the position of the marked isocenter (i.e., wires are not necessary for determining the beam geometry). The external fiducial markers indicating the marked isocenter are automatically detected as described previously.¹⁴ The initial version of this tool was developed for left-sided treatments only. Given the additional complexity of left-sided treatments because of the heart's proximity to the targets in these treatments, translating this approach to right-sided treatments should be easier than translating it in the opposite direction. Patient treatments were prescribed for a hypofractionated regimen of 40.05 Gy delivered in 15 fractions.¹⁵

The techniques for PMRT planning automation used algorithms developed in-house that were integrated with the Eclipse treatment planning system (Varian Medical Systems, Palo Alto, CA, USA) via its application programming interface. This PMRT planning tool is part of a suite of automated planning tools called the Radiation Planning Assistant that is being

developed to automate planning processes for resource-constrained clinics¹⁶ and currently includes treatment planning for radiotherapy of cervical and head and neck cancers.^{14,17} The inputs required by the Radiation Planning Assistant are a plan directive from the physician specifying the prescription and a CT scan for treatment planning. Another input needed for automatically planning PMRT is the location of the inferior border of the tangent. This additional user input is currently required because an automated technique for identifying this border that is sufficiently reliable has yet to be found, largely because of substantial variability between patients. Therefore, the user is required to identify the CT slice of the tangent fields' inferior border before automated planning is initiated.

The overall workflow for our automation technique for PMRT is illustrated in Fig. 1. After automatic segmentation of the targets, OARs, and additional planning structures are two main automated planning steps: (1) setting up the treatment beams and (2) optimizing the dose distributions. These steps are described in detail below. Once automated planning is completed, the user is presented with a composite treatment plan consisting of the tangential and SCV field plans, calculated dose, and heart and ipsilateral (left) lung contours, all of which are created automatically. We also implemented a technique to automatically verify the quality of the treatment plan and determine when it deviates from standard quality metrics to flag these deviations to the reviewer of the plan.

2.A.1. Automation of segmentation—The first step in our planning process is to automatically segment various anatomic structures, including the targets (chest wall and lymph nodes), several OARs (e.g., both lungs, heart, spinal canal), and other structures useful in defining beam geometry (e.g., sternum, clavicle, trachea). Automated segmentation was done using a tool developed by our group and described in detail previously.¹⁸ In short, multiple atlases of patient contours are deformed to the target patient and combined by using fusion based on the Simultaneous Truth and Performance Level Estimation.¹⁹ These atlases were created by our group and consisted of 11 patient CT scans with contours. This multi-atlas segmentation approach has been successfully used for many other anatomic sites and has the benefit of being easily adapted for different anatomical sites by creating a new set of patient atlases with the desired contours.^{17,20,21}

2.A.2. Automation of beam setup—Once automatic segmentation was complete, the next step was to determine the CT slice of the isocenter, representing the match line between the tangential fields and the SCV field. This slice was initially placed at the inferior aspect of the clavicular head. From there, the posterior, non-divergent border of the tangential fields (the principal border of the tangents separating the chest wall from the OARs) was determined by using support vector machine classification. This technique was adapted from the work described by Zhao et al.¹² and assigned points within the contours to one of two classes: target (chest wall) and avoidance (heart, lungs, and contralateral breast). These classified points were used as inputs to the support vector machine to determine the optimal three-dimensional plane separating the two classes for each patient. This plane represents the posterior border of the tangential fields and can be used to derive the beam parameters for the medial and lateral tangential fields, including the gantry angles, collimator angles, and jaw/multileaf collimator (MLC) positions defining the posterior border. The collimator angle

is set to zero, and the posterior border is defined using the MLC. The anterior jaw is defined to provide 2 cm of flash from the projection of the body contour. The inferior jaw is defined at the projection of the slice of the body contour at the inferior border (which was previously defined manually).

The first step in defining the SCV beam parameters after automatic segmentation was to determine the optimal medial border separating the targets (SCV lymph nodes) from the avoidance tissues (trachea and spinal canal). Again, a support vector machine was used to find the optimal plane, and this plane was used to define the gantry angle and medial jaw/MLC positions of the SCV field. Finally, the superior jaw was determined based on the beam's eye view (BEV) projection of the cricoid cartilage, and the lateral jaw and MLC positions for humeral head blocking were determined based on the BEV projection of the humeral head.

In some cases, the location of the match line (and isocenter in the superior-inferior direction) had to be automatically adjusted based on the patient's anatomy and beam geometry. If the tangential field length exceeded the machine capabilities (>20 cm for a Varian C-arm linear accelerator) or the part of the SCV field inferior to the humeral head was insufficient (<2 cm), the location of the match line was automatically adjusted toward the inferior direction, and planning continued. In some cases with excessive lung exposure in the SCV field (>4 cm based on the projection of the lung in the BEV), the match line was moved more toward the superior direction. In the latter case, two plans were created: the original plan with the match line at the inferior aspect of the clavicular head and an alternative plan with a more superior match line to reduce the amount of lung in the SCV field. The rationale for creating two plans was that several clinical factors contributed to the decision to move the match line, including the location of the level III axillary nodes and the possibility of the tangential fields intersecting part of the patient's arm. If upon reviewing the original plan the physician decides that moving the match line in the superior direction is advantageous, he or she can review the alternative match line plan. The alternative match line plans were created while still considering the constraints of maximum tangential field length and proximity of the match line to the humeral head. Fig. 2 illustrates an example of the resulting SCV field BEV for the original and alternative match line plans for one of the test patients.

2.A.3. Automation of dose optimization—Once the parameters for the open beams were determined, the three beams (medial and lateral tangents and SCV) were automatically generated in the treatment planning system and calculated for both 6- and 18-MV photons. Next, the dose per beam was exported and used as inputs for optimizing the dose distribution to reduce the maximum dose in the plan and the doses to OARs while maintaining target coverage. First, a normalization volume was created for each plan (tangential and SCV). These normalization volumes were derived from the automatic segmentations of the target structures (chest wall for the tangential plan and SCV and level III axillary lymph nodes for the SCV plan) that fell within the limits of the treatment fields. The normalization volumes were used to ensure that coverage was maintained throughout the optimization such that 95% of the normalization volume received 95% of the prescribed dose.

In the optimization of the dose distribution, the relative weights of the high-and low-energy beams were determined first for the open fields by using a brute-force search strategy. This optimization strategy allowed us to enforce the coverage of the normalization volume while selecting combinations of beam weights that met OAR dose constraints and minimized the maximum dose. Next, for the tangential fields, FIF segments were created by positioning the MLCs to block the projection of the hot dose cloud within each BEV, mimicking a forward-planning methodology. The dose of the hot spot to be blocked was determined adaptively based on the current maximum dose in the optimization (usually less than the maximum dose by 2% to 6% of the prescription) and the relative size of the hot dose cloud in the BEV (to prevent excessive blocking). The beam energy of each FIF segment and relative weighting were also determined by using another brute-force search. The process of creating FIF segments for the tangents was repeated one time if the maximum dose in the plan was greater than 110% of the prescription. The final resulting plans could have at most two SCV fields (high-and low-energy fields, no FIF segments) and four tangential field segments per beam angle (high-and low-energy open fields, two FIF segments). Combining the FIF segments with the open fields would result in a maximum of six treatment beams (two SCVs, two medial tangents, and two lateral tangents).

2.B. Evaluation of automated treatment planning

The performance of the automated planning tool was evaluated by using scans from a sample of 10 patients who underwent left-sided mastectomy and a free-breathing CT scan for radiotherapy planning at a partner hospital in South Africa. These CT scans were acquired with the patient in the head-first, supine position on a breast board with both arms raised over the head. All patients had external fiducial markers indicating their marked isocenters. Some patients had additional wires placed for treatment planning, although the wires were not used in this study. The average separation of the chest wall for these patients was 25.4 cm (range: 18.2–35.4 cm). These patients' CT scans were not used during algorithm development or preliminary testing of the automatic planning tool. All patient data used in this study were handled in accordance with an approved institutional protocol.

2.B.1. Validation of automatic segmentation—Although our automated techniques for PMRT planning make use of several automatically segmented structures for creating treatment plans, only the heart and ipsilateral (left) lung are presented with the plan. Therefore, the accuracy of segmentation of these contours was validated by comparing the automatically generated contours with physician-approved, manually edited contours. The physician-approved contours were created by using our automatic segmentation tool and then edited manually and reviewed and approved by a radiation oncologist (S.F.S.) with expertise in treatment of breast cancer. The contours were created according to the guidelines provided in the Breast Cancer Atlas for Radiation Therapy Planning from the Radiation Therapy Oncology Group.²² The contours were compared geometrically by using the Dice similarity coefficient, mean surface distance, and Hausdorff distance and dosimetrically by using differences in dose metrics for each set of contours from the automatically planned treatments.

2.B.2. Assessment of the automatically created treatment plans—Once the automatically created plans were ready in the treatment planning system, they were reviewed for acceptability for treatment by two radiation oncologists with expertise in the treatment of breast cancer (D.A. and T.T.) at Groote Schuur Hospital (Cape Town, South Africa). The plans were rated on a three-tiered scale: use plan as is, use plan with minor changes, and plan requires major changes. The specific changes requested for each plan were recorded. If a physician requested to see the alternative match line plan for a patient, that plan was shown to the physician (if it had been created), and the physician selected the preferred plan. The physicians' final plan ratings were reported for their selected preferred plans.

The selected plans were also assessed quantitatively for compliance with dose objectives for target coverage, OARs, and maximum plan dose. These dose objectives were evaluated by using the physician-approved, manually edited contours. Coverage of the following target structures was assessed: the chest wall, SCV lymph nodes, and level III axillary lymph nodes. The preferred dose objectives and acceptable dose limits used for evaluation of the targets and OARs are presented in Table I. These objectives were determined according to several sources, including recommendations from The Royal College of Radiologists,¹⁵ objectives from the Alliance A221505 clinical trial of hypofractionated PMRT (unpublished protocol),²³ and clinical constraints from collaborating institutions. Maximum doses were assessed separately for tangential and SCV field plans (preferred maximum dose <112% of the prescription) as well as for the composite plan (preferred maximum dose <116% of the prescription).

2.C. Automated verification of PMRT plan quality

In the preliminary testing of the automated PMRT planning techniques, plans were most commonly rejected because of their dosimetric properties rather than the geometric design of the beam setup. As a result, automated verification of the dose distribution was integrated into the automated PMRT planning tool to alert the plan reviewer to these potential dosimetric deviations, with alert thresholds set based on published dose objectives or clinic-specific objectives. These thresholds included maximum plan doses and doses to OARs. Additional verifications included those of the amount of lung projected in the BEV of the SCV and beam properties, such as the SCV gantry angle (Table II). The ability of these verification tests to detect potential deviations in the quality of the automatically planned treatments was evaluated for the 10 patient CT scans evaluated in this study.

3. RESULTS

3.A. Validation of automatic segmentation

The results of the geometric comparison of the automatically generated and physician-approved contours of the heart and ipsilateral lung are shown in Fig. 3. The Dice similarity coefficient values were all at least 0.85 for the heart and 0.93 for the ipsilateral lung, indicating very good agreement. We also observed good agreement of the mean surface distance, with all values less than 0.5 cm for all contours. The greatest differences between the automatically generated and physician-approved contours, as indicated by the larger

Hausdorff distances, occurred when one contour included more slices in the superior or inferior direction than the other.

The differences in the dose metrics when evaluated on the physician-approved contours compared with the automatically generated contours of the heart and ipsilateral lung are also shown in Fig. 3. The differences were all small, resulting in less than a 1 Gy difference in mean dose and less than a 2% difference in volume for the dose-volume histogram metrics. Although the dose to the physician-approved contours did trend higher than the automatically generated contours, it did not affect whether a plan met the dose objectives for planning. This demonstrates that using the doses to the automatically generated contours is appropriate when reporting plan quality to the user. (Note: the doses reported in the sections below are those to the manually edited contours.)

3.B. Assessment of the automatically created treatment plans

Upon physician review of the final 10 automatically planned treatments, the physicians rated all plans either acceptable as is (50%) or with only minor changes (50%). Of these plans, four were the alternative plans, in which the physicians preferred that the match line be placed more superior to the original match line. For the 10 original plans, physicians requested to see an alternative match line plan for five patients. One of these patients was constrained by the tangential field length limit (>20 cm), so alternative plans were presented for the remaining four, all of which were preferred by the physicians. Physicians requested a total of seven changes for the five plans: adding a heart block to reduce the heart dose in two patients, reducing the maximum dose in the tangential plan for one patient with a large separation, and reducing the depth of nodal coverage to reduce the maximum dose in the SCV plan, reducing the lung dose, adjusting the superior border of the SCV field, and adjusting the SCV angle in one patient each.

The resulting dose metrics for the heart and ipsilateral lung, coverage of the targets, and maximum doses are shown in Fig. 4. Ninety percent of the plans met the acceptable objective for the heart, with 60% meeting preferred objectives, and all of the plans met the preferred objectives for the ipsilateral lung. Regarding target coverage, all of the plans met the preferred objective, in which 95% of the volume was covered by 95% of the prescribed dose. Eighty percent of the plans met the preferred objective for the maximum dose (<116% of the prescribed dose). The two patients' plans that exceeded this value had maximum doses less than 118% of the prescription dose that were caused by large chest wall separation and deep lymph node targets. The locations of the maximum doses were checked to ensure that they did not fall within the brachial plexus.

On average, we found that creation of one treatment plan took 38 min (range 28–52 min). For plans for which an alternative match line plan was automatically created based on the amount of lung in the SCV BEV, an average of 24 min (range 17–28 min) was added to the planning time. On average, the majority of the time went toward setting up the beams (19 min), contouring (11 min), and dose optimization (7 min).

3.C. Automated verification of PMRT plan quality

In their evaluation of the 10 treatment plans, physicians requested a total of seven changes (described above) plus five requests to review alternative match line plans. Of these 12 requests, 11 (92%) were detected by the automatic plan quality verification tests. The only requested change not detected was adjustment of the SCV field's superior border. The tests detected four additional potential deviations that the physicians did not request to be changed: two plans with slightly high heart doses, one plan with a slightly high ipsilateral lung dose, and one plan with a slightly large amount of lung in the SCV field. All four of these potential deviations were very close to the thresholds set for each test.

4. DISCUSSION

In this work, we demonstrated the clinical viability of our automated planning tool for radiotherapy for locally advanced breast cancer after mastectomy. We developed this tool with the goal of reducing the workload on the limited radiotherapy staff of resource-constrained clinics, such as those in LMICs.⁸ Such automated tools have the potential to reduce staff workloads and improve the reliability of treatment planning.²⁴ Investigators have shown that clinical implementation of automated planning for tangential breast irradiation can improve the efficiency and quality of treatment planning, even facilitating same-day treatments.^{9,25} We would expect an even greater gain in efficiency for automation of the complex PMRT necessary for advanced breast cancers, which are more common in LMICs owing to late-stage diagnosis. Some have also suggested that reducing the effort spent in treatment planning through automation could reduce the cost of radiotherapy programs.²⁶ Automation of PMRT planning is a major step toward improving treatment planning efficiency, especially given that breast cancer is one of the most common cancers in LMICs.

To our knowledge, this is the first automated treatment planning tool designed for PMRT, which uses tangential fields to irradiate the chest wall matched with an oblique en face beam to irradiate the SCV lymph nodes. Although some clinics may also include the internal mammary chain (IMC) lymph nodes in such treatment, this remains an area of controversy.²⁷ Treatment of the IMC increases the dose delivered to the heart and the risk of heart disease.²⁸ In the context of patients undergoing free-breathing treatments because of resource limitations in LMICs, the heart doses and risk of heart disease are even higher. For this reason, clinics may only treat the IMC if these nodes are suspected of being involved. Therefore, we designed our automated planning tool for a technique that irradiates the chest wall and SCV and level III axillary lymph nodes, and not the IMC lymph nodes.

Without using external markers to set up the beams, the automation algorithms determined the appropriate beam angles for the tangential fields in this test cohort. However, not using markers means that one manual input is required for treatment planning: the location of the inferior border of the tangential fields. In the user interface of our automated planning tool, this border is conveniently selected in the same workspace in which the CT scan is approved for automated planning, which should add negligible effort and time to the entire planning process. Also, clinicians may follow their typical process for marking the inferior border, such as placement of a wire, to facilitate their selection of this location. The patient CT

scans we tested here as well as those used previously in the development of this automated planning tool came from several different institutions. As a result, a variety of approaches for placing markers and wires were used for these patients, which did not seem to influence the performance of our algorithms in setting up the beams.

We also integrated a method into our automated planning tool to automatically alert reviewers of the PMRT plan to any potential discrepancies in plan quality, which mainly resulted from the plan's dose distribution. Given the proximity of the targets to sensitive normal tissues and the variations in patient anatomy, balancing normal tissue sparing and full target coverage is sometimes a challenge in radiotherapy for breast cancer. We designed our automated treatment planning tool to create plans with full coverage of the target volumes. Therefore, this automatic verification may be useful in alerting the plan reviewer to potential discrepancies in plan quality, such as high heart dose, which may call for adjustment of the plan depending on the acceptable clinical compromises for that particular patient and plan. The alerts generated by the automatic plan quality verification tests could help expedite adjustment of treatment plans if necessary and improve the safety of automated treatment planning by automatically alerting the plan reviewer to potential issues with the plan.

The current version of this automated planning tool for PMRT designs radiation treatments based on specific clinical practices that may vary by institution, including patient positioning (supine, both arms up), the use of free-breathing scans, the location of the match line or superior border of the SCV field, and a hypofractionated treatment regimen. However, the automation techniques presented herein can be easily adapted to comply with variations in this clinical practice. Some variations in practice may require greater adaptations in the automation technique, but are still feasible. One example is the use of a single-energy photon beam, which is common in many clinics, rather than a mix of high-and low-energy beams. With adaptation, automation of PMRT with a single-energy photon beam is very likely possible, although the dose distributions for many patients would be expected to be hotter than those with mixed-energy photon beams. Another possible adaptation is using tangential and SCV fields for the treatment of intact breast and at-risk nodes. By changing the automatic segmentation to create the breast contour to use as the target for the tangents rather than the chest wall, the automation techniques would function the same as those used for planning PMRT. Before clinical implementation, all of these adaptations would need to be tested thoroughly.

In the evaluation described herein, we retrospectively planned PMRT treatments for a small cohort of patients with locally advanced breast cancer after mastectomy that required only minor changes or were acceptable for treatment as is. We also found that the automatic segmentation of the heart and ipsilateral lung was sufficiently accurate for presentation to the end user. A limitation of this work was the small number of patient datasets available for testing, which was a result of the limitations of data sharing agreements among the collaborating institutions. During development of the algorithms presented here, we were able to test earlier versions of the automated planning tool on 29 patient CT scans. We then used 10 previously untested CT scans for testing the final version (presented here). Moving forward, we will subject this automated planning tool to prospective testing with our

collaborating institutions before clinical implementation. In this prospective testing, we will compare automatically generated PMRT plans head-to-head with the corresponding manually created treatment plans.

The automated planning tool tested in this study was not optimized for time, and for some patients took as long as 52 minutes to create a plan. However, this is time that does not have to be spent by staff actively creating a treatment plan. After this study was completed and in preparation for clinical implementation, the tool was deployed on a network of servers that utilize parallel processes, a distributed calculation framework, and further improvements in computational speed. Based on preliminary data from testing this system, we estimate that the time to create a plan will be reduced to be less than 20 minutes for all patients.

Key considerations for clinical deployment of this automated treatment planning tool is ensuring that patient selection and setup are appropriate for the treatment technique planned by this automated tool. Thorough training will be necessary to ensure safe use and help users understand the specifications of this system. During clinical implementation, we will collect data on planning times to quantify improvements in efficiency when using this automated planning tool.

5. CONCLUSIONS

We developed and tested an automated planning tool for PMRT and demonstrated its viability for implementation in resource-constrained clinics in LMICs. This tool has the potential to improve efficiency in planning these complex treatments for breast cancer.

ACKNOWLEDGMENTS

This work was supported by National Institutes of Health/National Cancer Institute grants UH2-CA202665, UH3-CA202665, and P30CA016672 (Clinical Trials Support Resource). The authors thank the African Cancer Institute and Varian Medical Systems for their support and Dr. Nataliya Kovalchuk (Stanford University) for her contributions to this work. They also thank Don Norwood from the Department of Scientific Publications and Christine Wogan from the Division of Radiation Oncology at The University of Texas MD Anderson Cancer Center for editing this work.

REFERENCES

1. Ferlay J, Soerjomataram I, Dikshit R, et al. Cancer incidence and mortality worldwide: Sources, methods and major patterns in GLOBOCAN 2012. *Int J Cancer*. 2015;136(5):E359–E386. doi:10.1002/ijc.29210 [PubMed: 25220842]
2. Shulman LN, Willett W, Sievers A, Knaul FM. Breast Cancer in Developing Countries : Opportunities for Improved Survival. *J Oncol*. 2010;2010:1–6. doi:10.1155/2010/595167
3. Overgaard M, Jensen M-B, Overgaard J, et al. Postoperative radiotherapy in high-risk postmenopausal breast-cancer patients given adjuvant tamoxifen: Danish Breast Cancer Cooperative Group DBCG 82c randomised trial. *Lancet*. 1999;353(9165):1641–1648. doi:10.1016/S0140-6736(98)09201-0 [PubMed: 10335782]
4. Overgaard M, Hansen PS, Overgaard J, et al. Postoperative Radiotherapy in High-Risk Premenopausal Women with Breast Cancer Who Receive Adjuvant Chemotherapy. *N Engl J Med*. 1997;337(14):949–955. doi:10.1056/NEJM199710023371401 [PubMed: 9395428]
5. Ragaz J, Olivetto IA, Spinelli JJ, et al. Locoregional Radiation Therapy in Patients With High-Risk Breast Cancer Receiving Adjuvant Chemotherapy: 20-Year Results of the British Columbia

- Randomized Trial. *J Natl Cancer Inst.* 2005;97(2):116–126. doi:10.1093/jnci/djh297 [PubMed: 15657341]
6. Poortmans PM, Collette S, Kirkove C, et al. Internal Mammary and Medial Supraclavicular Irradiation in Breast Cancer. *N Engl J Med.* 2015;373(4):317–327. doi:10.1056/NEJMoa1415369 [PubMed: 26200978]
 7. Zubizarreta EH, Fidarova E, Healy B, Rosenblatt E. Need for Radiotherapy in Low and Middle Income Countries – The Silent Crisis Continues. *Clin Oncol.* 2015;27(2):107–114. doi:10.1016/j.clon.2014.10.006
 8. Datta NR, Samiei M, Bodis S. Radiation therapy infrastructure and human resources in low-and middle-income countries: Present status and projections for 2020. *Int J Radiat Oncol Biol Phys.* 2014;89(3):448–457. doi:10.1016/j.ijrobp.2014.03.002 [PubMed: 24751411]
 9. Purdie TG, Dinniwell RE, Fyles A, Sharpe MB. Automation and intensity modulated radiation therapy for individualized high-quality tangent breast treatment plans. *Int J Radiat Oncol Biol Phys.* 2014;90(3):688–695. doi:10.1016/j.ijrobp.2014.06.056 [PubMed: 25160607]
 10. Purdie TG, Dinniwell RE, Letourneau D, Hill C, Sharpe MB. Automated Planning of Tangential Breast Intensity-Modulated Radiotherapy Using Heuristic Optimization. *Int J Radiat Oncol Biol Phys.* 2011;81(2):575–583. doi:10.1016/j.ijrobp.2010.11.016 [PubMed: 21237584]
 11. Fan J, Wang J, Zhang Z, Hu W. Iterative dataset optimization in automated planning: Implementation for breast and rectal cancer radiotherapy. *Med Phys.* 2017;44(6):2515–2531. doi:10.1002/mp.12232 [PubMed: 28339103]
 12. Zhao X, Kong D, Jozsef G, et al. Automated beam placement for breast radiotherapy using a support vector machine based algorithm. *Med Phys.* 2012;39(5):2536. doi:10.1118/1.3700736 [PubMed: 22559624]
 13. Chen G-P, Ahunbay E, Li XAA. Automated computer optimization for 3D treatment planning of breast irradiation. *Med Phys.* 2008;35(6Part1):2253–2258. doi:10.1118/1.2911869 [PubMed: 18649455]
 14. Kisling K, Zhang L, Simonds H, et al. Fully automatic treatment planning for external beam radiation therapy of locally advanced cervical cancer – a tool for low-resource clinics. *J Glob Oncol.* 2019:1–9. doi:10.1200/JGO.18.00107
 15. Postoperative Radiotherapy for Breast Cancer: UK Consensus Statements. The Royal College of Radiologist, London https://www.rcr.ac.uk/system/files/publication/field_publication_files/bfco2016_breast-consensus-guidelines.pdf. Published 2016. Accessed February 26, 2019.
 16. Court LE, Kisling K, McCarroll R, et al. Radiation Planning Assistant -A streamlined, fully automated radiotherapy treatment planning system. *J Vis Exp.* 2018;2018(134):e57411-e57411. doi:10.3791/57411
 17. McCarroll RE, Beadle BM, Balter PA, et al. Retrospective Validation and Clinical Implementation of Automated Contouring of Organs at Risk in the Head and Neck: A Step Toward Automated Radiation Treatment Planning for Low-and Middle-Income Countries. *J Glob Oncol.* 2018;4(4):1–11. doi:10.1200/JGO.18.00055
 18. Yang J, Zhang Y, Zhang L, Dong L. Automatic segmentation of parotids from CT scans using multiple atlases. In: *Medical Image Analysis for the Clinic: A Grand Challenge.*; 2010:323–330.
 19. Zou KH, Warfield SK, Bharatha A, et al. Statistical Validation of Image Segmentation Quality Based on a Spatial Overlap Index. *Acad Radiol.* 2004;11(2):178–189. doi:10.1016/S1076-6332(03)00671-8 [PubMed: 14974593]
 20. Zhou R, Liao Z, Pan T, et al. Cardiac atlas development and validation for automatic segmentation of cardiac substructures. *Radiother Oncol.* 2017;122(1):66–71. doi:10.1016/j.radonc.2016.11.016 [PubMed: 27939201]
 21. Yang J, Amini A, Williamson R, et al. Automatic contouring of brachial plexus using a multi-atlas approach for lung cancer radiation therapy. *Pract Radiat Oncol.* 2013;3(4):e139–e147. doi:10.1016/j.pro.2013.01.002 [PubMed: 24674411]
 22. White J, Tai A, Arthur D, et al. Breast Cancer Atlas for Radiation Therapy Planning: Consensus Definitions. Radiation Therapy Oncology Group <https://www.rtog.org/LinkClick.aspx?fileticket=vzJFhPaBipE%3D&tabid=236>. Accessed October 13, 2017.

23. Poppe M Hypofractionated radiation therapy after mastectomy in preventing recurrence in patients with stage IIa-IIIa breast cancer. 2017.
24. Moore KL, Kagadis GC, McNutt TR, Moiseenko V, Mutic S. Vision 20/20: Automation and advanced computing in clinical radiation oncology. *Med Phys.* 2014;41(1). doi:10.1118/1.4842515
25. Amit G, Purdie TG. Automated planning of breast radiotherapy using cone beam CT imaging. *Med Phys.* 2015;42(2):770–779. doi:10.1118/1.4905111 [PubMed: 25652491]
26. Atun R, Jaffray DA, Barton MB, et al. Expanding global access to radiotherapy. *Lancet Oncol.* 2015;16(10):1153–1186. doi:10.1016/S1470-2045(15)00222-3 [PubMed: 26419354]
27. Recht A, Comen EA, Fine RE, et al. Postmastectomy Radiotherapy: An American Society of Clinical Oncology, American Society for Radiation Oncology, and Society of Surgical Oncology Focused Guideline Update. *J Clin Oncol.* 2016;34(36):4431–4442. doi:10.1200/JCO.2016.69.1188 [PubMed: 27646947]
28. Taylor CW, Wang Z, Macaulay E, Jagsi R, Duane F, Darby SC. Exposure of the Heart in Breast Cancer Radiation Therapy: A Systematic Review of Heart Doses Published During 2003 to 2013. *Int J Radiat Oncol Biol Phys.* 2015;93(4):845–853. doi:10.1016/j.ijrobp.2015.07.2292 [PubMed: 26530753]

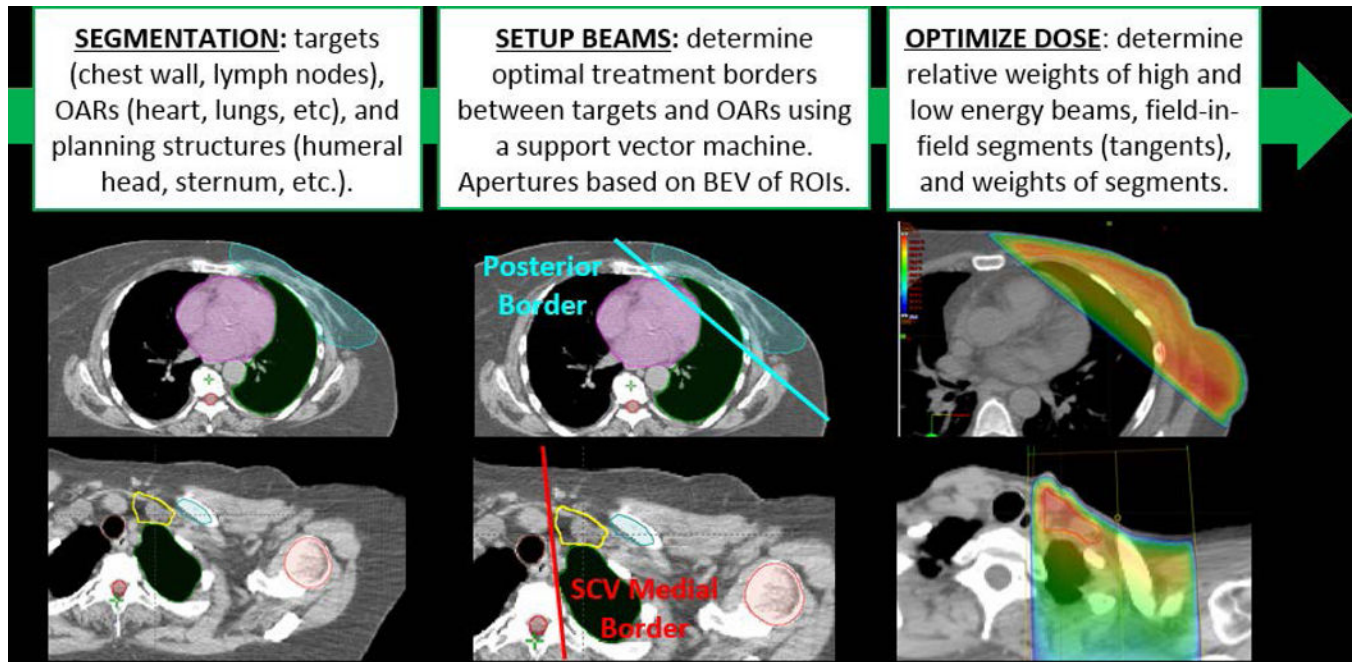


Fig. 1. Overview of the method for automated planning of postmastectomy radiotherapy. OARs, organs at risk; BEV, beam's eye view; ROIs, regions of interest.

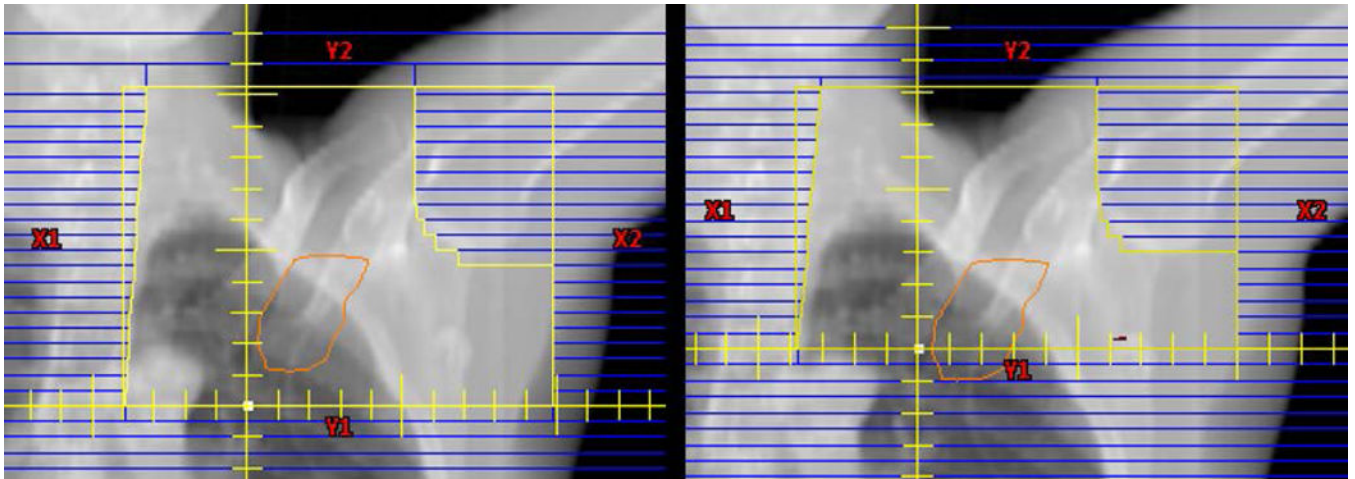


Fig. 2. Beam's eye view of supraclavicular fields for the original match line plan (left) and alternative match line plan (right) for the same patient. The contour of the level III axillary nodes are shown projected in orange.

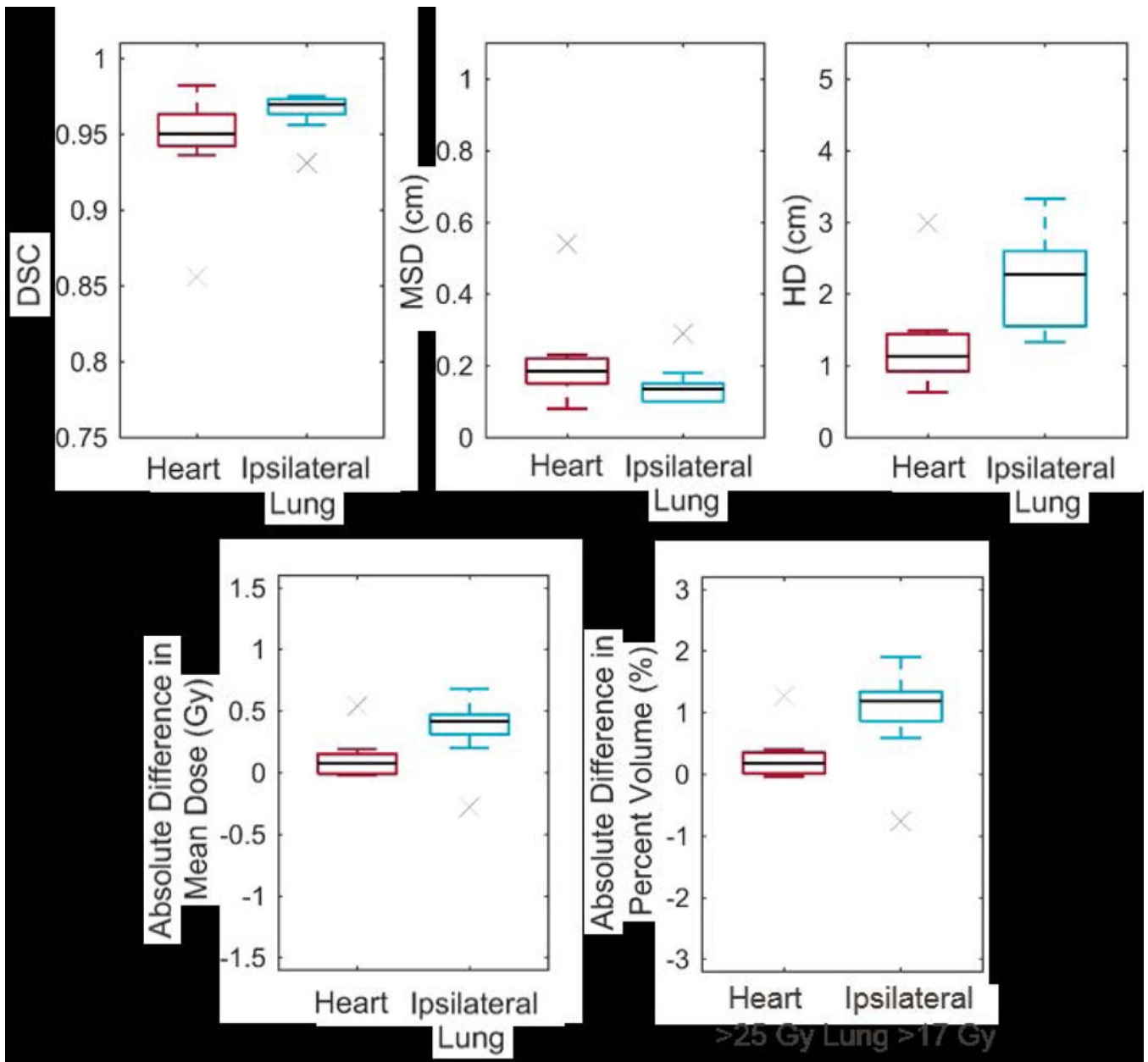
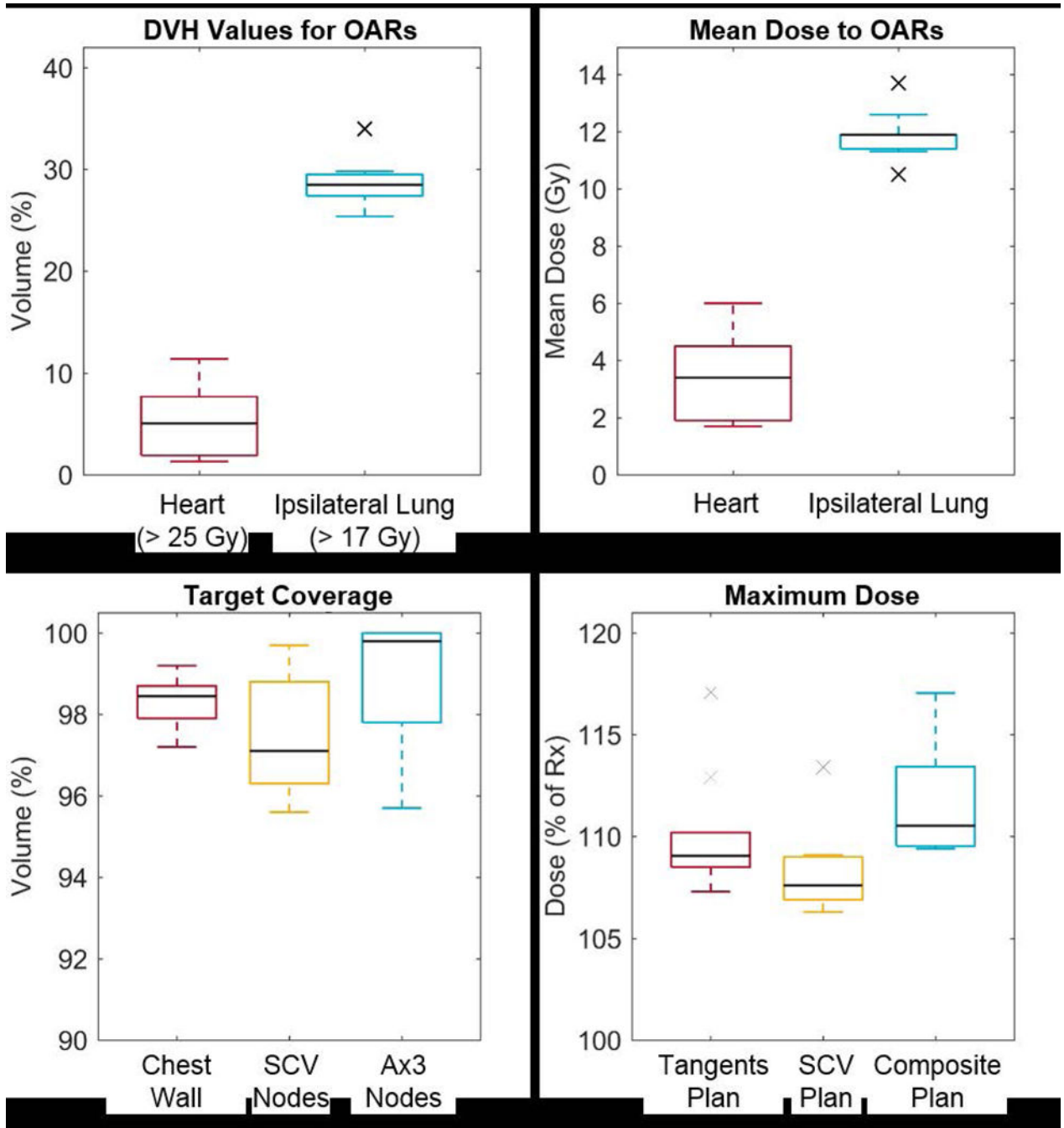


Fig. 3.

Comparison of the automatically generated and physician-approved contours of the heart and ipsilateral lung. The top row shows the following results of the geometric comparisons: Dice similarity coefficient (DSC; left), mean surface distance (MSD; center), and Hausdorff distance (HD; right). The bottom row shows the following results of the dosimetric comparisons: mean OAR dose (left) and dose-volume histogram metric (right). The absolute difference in metrics was the results for the physician-approved contour minus that for the automatically generated contour for the same plan.

**Fig. 4.**

The final dose metrics for the 10 automatically planned treatments. The dose-volume histogram (DVH) metrics (top left), mean dose delivered to the heart and ipsilateral lung (top right), coverage of targets by 95% or the prescription dose (bottom left), and maximum doses for the tangential and SCV plans and for a composite of the two plans (bottom right) are shown. OARs, organs at risk; SCV, supraclavicular; Ax3, level III axillary; Rx, prescription.

Table I.

Hypofractionated PMRT dose objectives for target coverage and organs-at-risk

Structure	Dose metric	Preferred objective	Acceptable limit
Targets	Volume >95% Rx	>95%	n/a
Targets	Volume >90% Rx	n/a	>90%
Heart	Mean dose	<4 Gy	<6 Gy
	Volume >25 Gy	<7%	<10%
Ipsilateral lung	Volume >17 Gy	<35%	<40%

Rx, prescription; n/a, not applicable.

Author Manuscript

Author Manuscript

Author Manuscript

Author Manuscript

Table II.

Thresholds for automated verification tests of automated PMRT plan quality

Test object	Test metric	Threshold
Maximum dose (composite)	Point dose	>116% of prescription
Maximum dose (tangential plan)	Point dose	>112% of prescription
Maximum dose (SCV plan)	Point dose	>112% of prescription
Heart dose	Mean dose	<4 Gy
	Volume >25 Gy	<7%
Ipsilateral lung dose	Volume >17 Gy	<30%
Lung in SCV field	Projection height	<4 cm
SCV gantry angle	Angle off vertical	>15°

Author Manuscript

Author Manuscript

Author Manuscript

Author Manuscript